MISR JOURNAL OF AGRICULTURAL ENGINEERING
https://mjae.journals.ekb.eg/
ISSN-Print: 1687-384X
ISSN-Online: 2636-3062
Misr J. Ag. Eng., 42 (---): ….. - …..
DOI: 10.21608/mjae.2025.411071.1162

EFFECT OF USING AN ELECTROMAGNETIC FIELD ON THE PERFORMANCE OF REVERSE OSMOSIS MEMBRANES IN BRACKISH WATER

S.T. Abd El Aziz[1&*], O.M. Bedair[2], A. Mossad [2], H.E. Ahmed[3], K.M. El Sawah[4], A.M.M. Salama[5]

[1] MSc Stud. in Ag. Eng. Dept., Fac. of Ag., Ain Shams U. Qalyubia, Egypt.
[2] Prof. of Ag. Eng. Dept., Fac. of Ag., Ain Shams U. Qalyubia, Egypt.
[3] Consultant to the Chairman of the Board of the Engine Factory, AOI, Cairo, Egypt.
[4] Freelance Electronics Engineer. Cairo, Egypt.
[5] Lect. of Soil Sci. Dept., Fac. of Ag., Ain Shams U. Qalyubia, Egypt.
* E-mail: salwa_Tarek@agr.asu.edu.eg

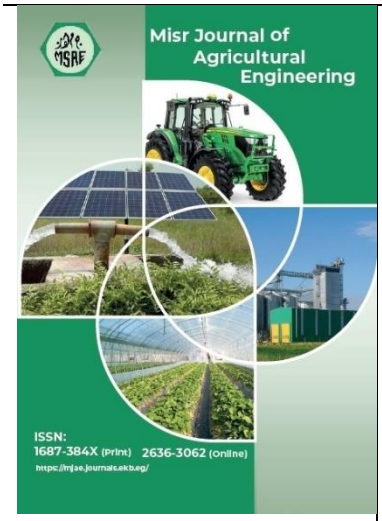

© Misr J. Ag. Eng. (MJAE)

Keywords:
Desalination; Brackish water; Reverse Osmosis (RO); Membrane Scaling; Electromagnetic Field (EMF); Frequency Generator; Water Recovery rate; Salt Rejection rate; Estimation Elements

ABSTRACT

Reverse osmosis membranes have long been one of the most popular and effective methods for desalination, due to their ease of operation and high efficiency in salt separation. However, scaling remains one of the most significant challenges associated with these membranes, as it can reduce flow rates and cause membrane damage. Therefore, over the decades, the electromagnetic field has been widely used in water treatment processes to address such issues. This study involved two experiments: the first was conducted without the application of an electromagnetic field before the membrane, and the second with an electromagnetic field applied before the membrane. Both experiments were conducted in the research laboratory of the Department of Soil and Water Sciences, Faculty of Agriculture, Ain Shams University.

The objective of the study was to investigate the effect of an electromagnetic field generated through a coil of electrically conductive wire, powered by a frequency generator circuit operating at 150 kHz. The results showed an increase in salt rejection in the freshwater outlet, a decrease in sodium and chloride ions in both the freshwater and concentrate streams (as determined by elemental analysis), and a reduction in the percentage of freshwater recovery.

INTRODUCTION

The global water situation is concerning and expected to deteriorate over time due to increasing freshwater scarcity. Currently, around one billion people lack access to clean and safe drinking water, and this number is projected to rise significantly in the coming years. Membrane processes, particularly reverse osmosis, are expected to gain popularity in water treatment applications due to their high purification efficiency and energy efficiency compared to other technologies **(Geise et al., 2010).**

Brackish water desalination using reverse osmosis (BWRO) is now widespread in areas with abundant brackish groundwater, such as the United States and North Africa **(Pearson et al.,**

2021). Membrane modules that are sold commercially include hollow fiber, spiral wound, plate and frame, and tubular **(Nair and Kumar, 2013).** Spiral-wound membrane modules are currently the most widely used type for reverse osmosis (RO) due to their high packing density (**Taherinejad et. al., 2017)**. Scaling is a common challenge faced by reverse osmosis (RO) membranes in potable reuse applications due to elevated product recovery rates (**Lee et al., 2020**), while **Antony et al**. (2011) mentioned that despite the availability of various scale prediction tools and numerous scale mitigation measures used in the water treatment industry.

Scaling occurs when sparingly soluble salts are deposited. Dissolved inorganic substances such as Calcium (Ca^{+2}), Magnesium (Mg^{+2}), Carbonate (CO_3^{-2}), Sulfate ($SO4^{-2}$), Silica, and Iron can precipitate as insoluble salts, or scales, on the membrane surface if their solubility limits are exceeded **(Sheikholeslami, 2004).** A phenomenon arises whenever the solubility limits of sparingly soluble salts in the feed water are exceeded, highlighting the critical impact of solubility on system performance **(Antony et al., 2011).**

Scaling can lead to several significant challenges, including a decline in flux, damage to the membrane, reduced solute rejection and an increased passage of salt into the permeate**.** Recognizing these symptoms is crucial for maintaining optimal system performance and preventing long-term damage **(Chen et. al., 2020)**. When minerals dissolve or remain suspended in a solution, they tend to precipitate and gravitate towards the membrane surface due to their inherent charges **(Bisbee, 2003 and Thompson et al., 2012).** Scaling characterized by crystal formation poses a significant risk to the integrity of the active membrane layer, potentially resulting in damage that undermines performance **(Conway, 2002).**

Enhancing membrane durability and lifespan is crucial for affordability. The polymer used must be strong enough to endure harsh environments for many years **(Geise et al., 2010).** Managing membrane fouling and scaling is crucial for cost-effective treatment and long-term system resilience **(Penteado de Almeida et. al., 2023).**

The expense is also greatly increased by pre-treatment because membrane pre-treatment significantly lowers (RO) maintenance and operation costs and works well in open water intake facilities, it is gaining popularity despite conventional pre-treatment requiring less capital investment **(Greenlee et al., 2009).** Current scale control techniques include pretreatment with acid and antiscalants, although chemical treatments can alter the water's composition and result in hazardous byproducts. Cleaning remains the most widely used management approach (**Lee et al., 2010; Schoenbach et. al., 1996**).

However, there are several significant drawbacks to chemical cleaning (RO) membranes, including the membranes' shortened lifespan, high cost, and potential environmental risks. Additionally, as this review discusses, feed spacers typically inhibit the chemicals' ability to fully extract the inactivated material. The leftover biomass causes biofilms to rebuild quickly, requiring more frequent cleaning operations **(Matin et al., 2021).** Additionally, this could be harmful to the environment or people **(Antony et al., 2011**). However, if ion concentrations are high, antiscalants cannot prevent scaling, and precipitation will eventually happen when salt concentrations rise **(Greenlee et al., 2009).** Since prevention is encouraged over cleaning, non-chemical techniques and tools might be beneficial for preventing scaling and biofouling **(Lin et al., 2020).** Especially, magnetic treatment is divided into three categories: magnetic (permanent/electromagnetic), electrostatic, and alternating current (AC) induction (**Huchler et**

al., 2002). Magnetic treatment can be combined with other desalination and water treatment processes to enhance their effectiveness. For instance, when magnetic treatment is integrated with reverse osmosis (RO), it creates an improved RO desalination method. Additionally, magnetic separation can be used for anticaking treatment instead of desalination. In many cases, incorporating magnetic separation has resulted in improved performance of these processes. A magnetic field (MF) is applied to saline water, resulting in various changes to the treated water. This application weakens the hydrogen bonds between water molecules and dissolved ions, facilitating the separation process. The magnetic field can be generated using either a permanent magnet or an electromagnet **(Alwan et al., 2024).** The process of magnetization effectively reduces water hardness, which is primarily responsible for scale buildup, by limiting the presence of CO_3^{-2} and Ca^{+2} ions that contribute to the formation of $CaCO_3$ particles **(Saksono et al., 2011).** Using permanent magnets in magnetic desalination offers low operating costs; however, the effectiveness of this method can decline over time. In contrast, electromagnetic desalination incurs higher operating costs because it requires an electrical supply to maintain the magnetic field and a cooling water supply to prevent the solenoid from overheating. Despite the increased costs, electromagnetic desalination is more stable and effective than using permanent magnets **(Alwan et al., 2024).** However, electromagnetic fields (EMF) offer a highly effective, cost-efficient, and energy-saving solution for preventing scaling in reverse osmosis (RO) systems. By utilizing this innovative technology, you can significantly enhance system performance while reducing operational costs **(Du et al., 2025).** Because of its ease of use and minimal or nonexistent energy requirements, electromagnetic field (EMF) treatment is a viable method for controlling scaling. According to the study, $CaCO_3$ precipitation was encouraged in bulk solutions by even weak EMFs (such as magnetic fields <0.03 mT and electric fields <0.15 V/m) **(Du et al., 2024).** By using EMF with a spiral wound (RO) unit, noted improvements in permeate flow rate and salt rejection **(Rouina et al., 2016).**

This study aims to enhance the performance of reverse osmosis membranes and improve the quality of treated brackish water by investigating the effects of applying an electromagnetic field during the desalination process.

MATERIAL AND METHODS

3.1 Brackish Water Quality

The experiments were conducted at the Laboratory of the Soil and Water Department, Faculty of Agriculture, Ain Shams University, to perform a chemical analysis of the brackish water entering the system, which had a salinity of 4.050 $dS \cdot m^{-1}$. The results of the dissolved solids estimation in the feed water are presented in Table (1).

Table 1: Soluble cations and anions of brackish water (feed water).

pH	EC ($dS.m^{-1}$)	Soluble cations ($meq.l^{-1}$)				Soluble anions($meq.l^{-1}$)			
		Ca^{2+}	Mg^{2+}	Na^{+}	K^{+}	Cl^{-}	CO_3^{2-}	HCO_3^{-}	SO_4^{2-}
6.0	4.050	2.80	4.40	7.95	25.35	35.00	n.d	1.90	3.60

3.2. Pilot-Scale (RO) System

Fig. (1) illustrates the desalination water system, which consists of a reverse osmosis (RO) unit containing RO membrane elements (LMP-2012-100, India) with dimensions (length, outer diameter, inner diameter) (298 mm, 47 mm, 17 mm) designed for moderately brackish water, with a discharge capacity of 100 GPD and capable of rejecting impurities as small as 0.0001

microns, with maximum TDS 4000 Ppm, with maximum testing pressure 689.47 kPa. The system is equipped with two pumps: one for feeding (1.2 LPM – 861.84 kPa – 24 V) and the other for providing the necessary pressure for membrane operation (1.6 LPM – 861.84 kPa – 24 V). Additionally, the system includes three cartridge filters for pre-treatment of the water before it enters the membrane, to remove particulates and other macromolecules. The first is a sediment filter (removes particles up to 5 microns), the second is a granular activated carbon filter, and the third is a carbon block filter. Both carbon filters are used to reduce the chlorine content in the brackish feed water. Water flows through plastic pipes with a diameter of 4 mm. After (RO) desalination, the water is divided into two streams: the first is low-salinity fresh water, and the second is concentrated brine (high-salinity water), as shown in Fig. (1).

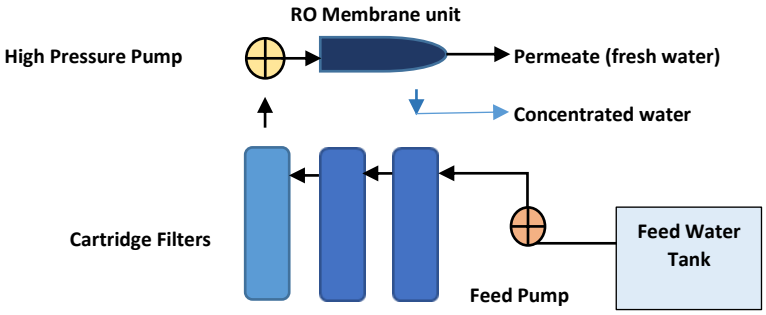

Fig. 1 : **Schematic diagram of the brackish water reverse osmosis (RO) desalination system**

A new membrane and new cartridge filters were used for each experiment separately over a total period of 150 hours. The same prepared feed water was introduced into the system in both experiments, with a constant feed flow rate of 1.0 $L \cdot min^{-1}$. In the first experiment, conducted without an electromagnetic field (EMF), the water passed through the cartridge filters and then into the membrane, as shown in Fig. (1). In the second experiment, the water passed through a coil that generated an electromagnetic field before entering the membrane directly, as shown in Fig. (3).

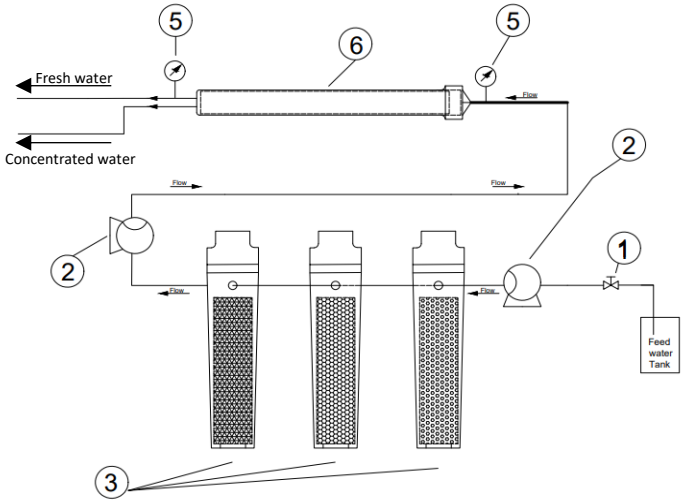

1-Valve
2-Diaphragm pump
3-Cartridge filter

Fig. 2: Schematic diagram of the brackish water desalination RO system without EMF

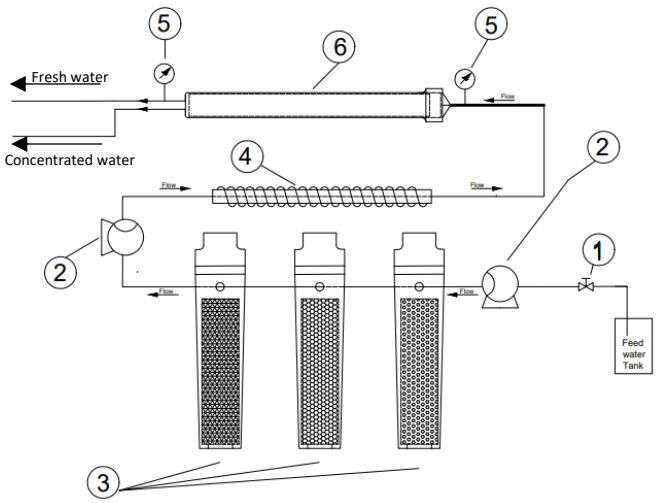

4- Electromagnetic coil
5-Pressure gauge
6-RO membrane unit

Fig. 3: Schematic diagram of the brackish water desalination RO system with EMF (second experiment)

3.3. Electro-Magnetic Flow Device

Fig. (4) shows the solenoid made of electrically conducting wire (coil) used to generate a magnetic field within its cavity when an electric current passes through it. The solenoid was manufactured by wrapping four layers (148 turns) of copper braided conductor around an iron pipe with a diameter of 4 mm. The electromagnetic field (EMF) was generated by connecting the two ends of the wire to a frequency generator circuit, where (+12 volts) flowed through one end and (-12 volts) through the other. The power consumption was 1.22 Watts, as calculated using Equations (1) and (2) according to **Beaty, (2001):**

$$\text{Electric Power (for AC circuit)} = \frac{V^2}{Z} \quad (1)$$

$$Z = \sqrt{R_t^2 + \omega^2 L^2} \quad (2)$$

Where: V : voltage (V),
Z : impedance (ohms),
Rt : conductor resistance (ohms),
ω : radial frequency (rad.μs-1),and
L : electrical inductance (μH).

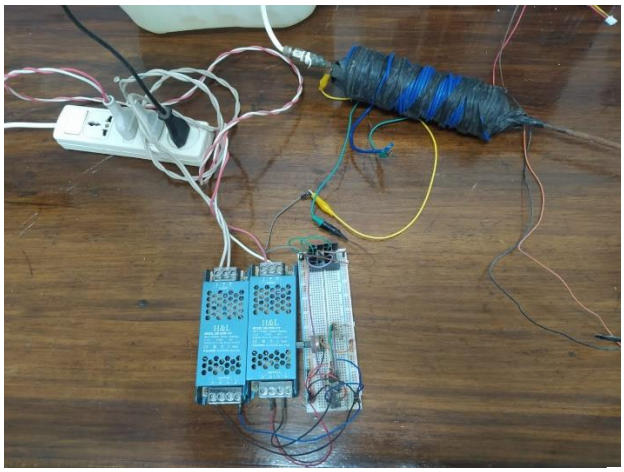

Fig. (4): The EMF unit in reality

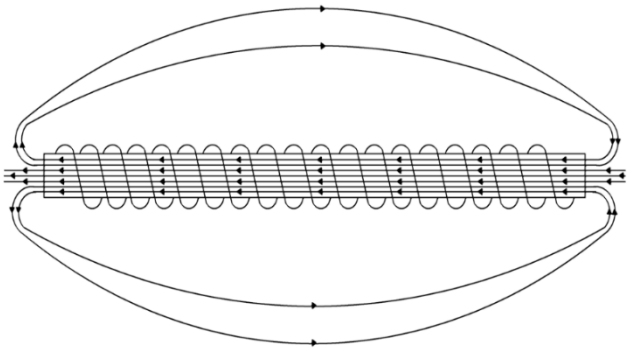

Fig. (5): Schematic diagram of the magnetic field waves

3.3.1. Frequency Generator Circuit

The solenoid requires a driving circuit to generate electromagnetic waves. To achieve this, it is necessary to vary the frequency of the current passing through the solenoid. This was accomplished by designing a frequency generation circuit, as illustrated in Fig. (6), which consists of several components, including:

1- An operational amplifier **(**TL071 IC). The most important parameter of the op-amp in this application is the slew rate, which refers to the maximum rate at which the output voltage of the op-amp can rise or fall.

Since the circuit operates with a dual power supply of ±12 VDC, the output voltage swing is considered equal to the waveform amplitude (A). The circuit is also designed to operate at a maximum frequency (f) of 150 kHz. Therefore, the selected op-amp must have a minimum slew

rate of at least 12 V/μs. The value of slew rate was calculated from the following equations (3 , 4 and 5) according to **(Beaty, 2001** and **Razavi, 2021):**

$$V = Asin(\omega t) \quad (3)$$

$$\omega = 2\pi f \quad (4)$$

$$max(slew\ rate) = A\ \omega \quad (5)$$

Where: $V(t)$: output voltage with respect to time (v.μs-1),

A: output voltage amplitude (V),

ω: radial frequency (rad.μs-1), and

t: time (μs).

The TL071 operational amplifier has a slew rate of 13 V.μs-1, which is suitable for our application.

2- A network of passive components, in which the op-amp is configured as a Wien Bridge Oscillator. This circuit is capable of generating a sine wave with frequencies of up to approximately 200 kHz.The operating frequency can be controlled using a network of passive components (resistors, capacitors, and inductors). However, to keep the design simple, only resistors and capacitors were used, and only two values of each component were required. The operating frequency (f) is determined using a network consisting of two resistors (R_1 and R_2) and two capacitors (C_1 and C_2). The frequency was calculated using Equation (6) according to **Razavi (2021)**.

$$f = \frac{1}{2\pi RC} \quad (6)$$

Where: f: the operation frequency (KHZ),

R : the resistor's value (ohms), and

C : the capacitor's value (farad).

The values of the two resistors are equal, and the values of the two capacitors are also equal, as shown in Fig. (6). Meanwhile, the amplitude of the output waveform is controlled by adjusting the input voltage.

3- A comparator stage using the LM339 was implemented to convert the output signal from the previous stage. As shown in Fig. (7), the previous stage produces a sine wave; however, the application requires a square wave, as illustrated in Fig. (8). Therefore, the comparator was used to perform the waveform conversion.

Fig. (9) displays the two types of waveforms generated by the circuit as observed on the oscilloscope (GDS-1102-U, Taiwan). A **c**omparator is an electronic device that compares two voltages or currents and outputs a digital signal indicating which input is higher. If the voltage at the positive terminal of the comparator exceeds that at the negative terminal, the output switches to the positive rail (i.e., the positive supply voltage, which is +12 V in this case). Otherwise, the output switches to the negative rail (–12 V). The LM339 comparator was selected for this application due to its ability to respond to signal variations as small as 1.3 μs.

In this setup, the sine wave output from the previous stage is connected to the positive terminal of the comparator, while a potentiometer is connected to the negative terminal. The potentiometer allows control over the output waveform’s pulse width using a technique known as pulse width modulation (PWM).

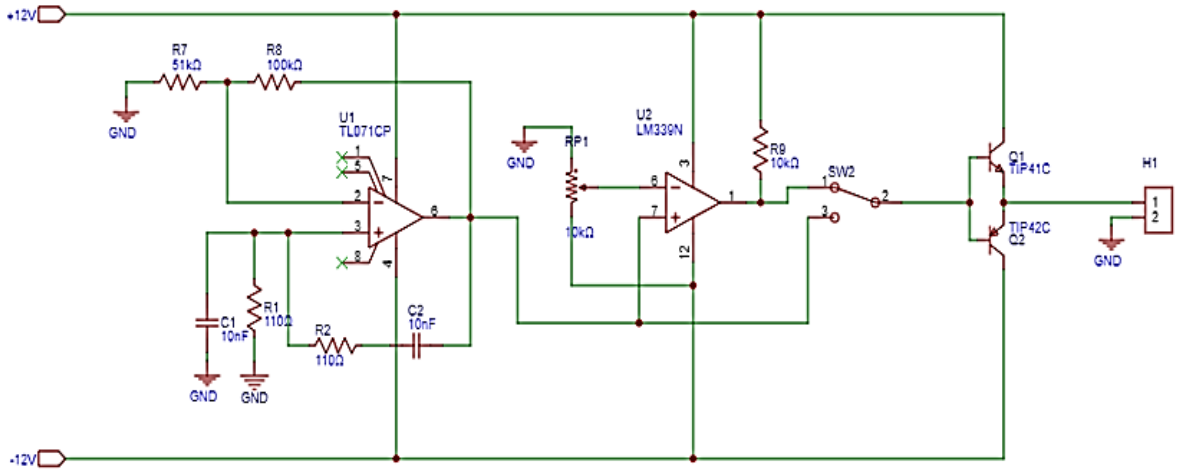

Fig. (6): Schematic diagram of frequency generator circuit.

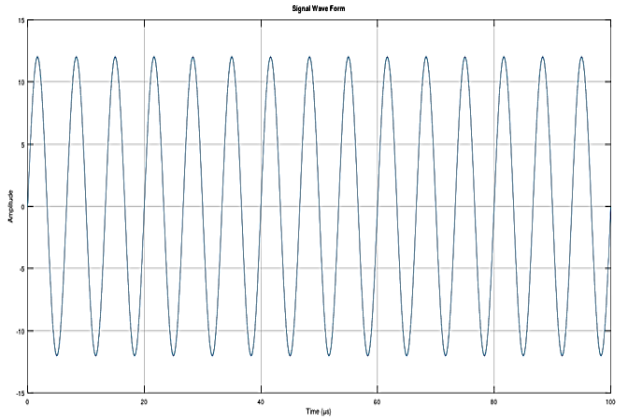

Fig. (7): Schematic diagram of sine waves.

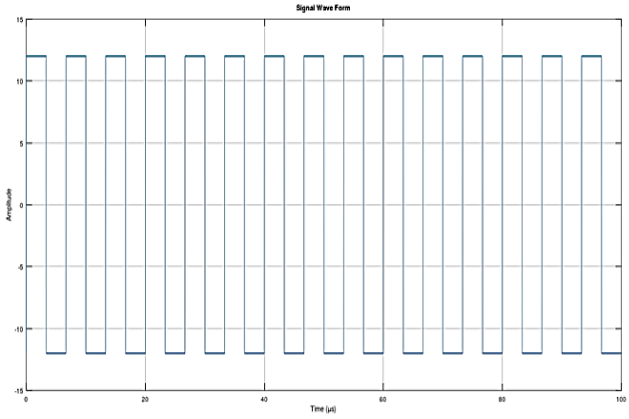

Fig. (8): Schematic diagram of square waves.

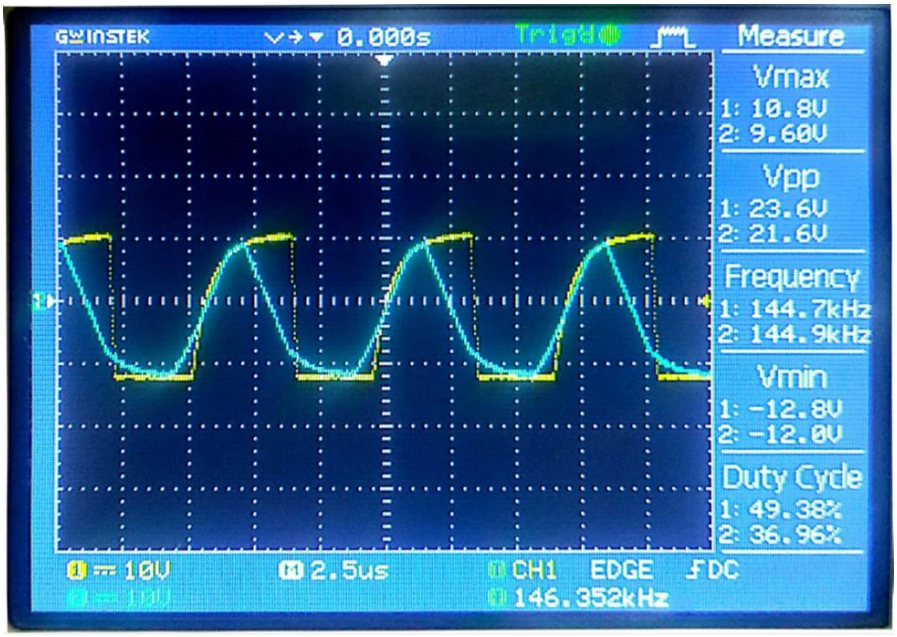

Fig. (9): Schematic diagram of Sine and Square waves on an Oscilloscope device.

4- Power Amplifier Stage: This stage is designed to provide the output waveform with sufficient power to operate the system effectively. It consists of two power transistors: one NPN transistor (TIP41) and one PNP transistor (TIP42). Together, they form a circuit known as a Class B power amplifier. This configuration operates using a push-pull mechanism, where one transistor functions as the push transistor and the other as the pull transistor. The push transistor increases the output voltage up to the maximum level (+12 V), while the pull transistor reduces it to the minimum level (−12 V). In this arrangement, each transistor conducts during only half of the signal cycle, which improves efficiency and enhances thermal performance by reducing power dissipation.

3.4. Measurements and Calculations

3.4.1 Measurements

3.4.1.1 Chemical Measurements

For each experiment, 11 samples of fresh outlet water and 11 samples of concentrated outlet water (as shown in Fig. (1)) were collected to investigate the effects of electromagnetic field (EMF) treatment on the membrane and to identify any notable differences between the experiments with and without EMF treatment. The evaluation focused on estimating specific elements (sodium [Na] and chloride [Cl]) as well as electrical conductivity (EC) over a period of 150 hours, with measurements taken every 6 hours in each experiment.

The measurements were obtained using both laboratory analysis and direct equipment readings:

- Dissolved sodium (Na^+) in each sample was measured using a flame photometer (CORNING M410, S/N 1656, UK) with an accuracy of ±0.01 $mg \cdot L^{-1}$.
- Dissolved chloride (Cl^-) was determined by volumetric titration, following the method described by **Skoog et al. (1996)**.
- Salinity of the feed water, fresh outlet water, and concentrated outlet water was measured by evaluating electrical conductivity (EC) using an EC meter (AD32, Adwa, Romania) with an accuracy of ±0.01 $dS \cdot m^{-1}$.
- The pH value was measured using a pH meter (pH-009(I), Pometer, China) with an accuracy of ±0.1 pH.

3.4.1.2 Hydraulic Measurements

- Pressure was measured before the membrane unit directly and after the membrane unit where the pressure gauge was installed on the freshwater line, over 150 hours (with measurements taken every 6 hours) for each experiment using a pressure gauge with a range of 0–1000 kPa and an accuracy of ±20 kPa
- Flow rate was also measured over 150 hours (every 6 hours) using a graduated cylinder. The measurement was performed by collecting a specific volume of discharged liquid in the cylinder (accuracy ±10 milliliters), and recording the time taken for that volume to be collected. The flow rate (Q) was then calculated using Equation (7), according to **Chase, (2022)**.

$$Q = \frac{V}{T} \quad (7)$$

Where: V: Volume timed at flowing conditions (Litre), and T: time (min).

3.4.1.3 Energy Consumption

Energy consumption and power of the entire system were analyzed using a power meter (UT230B-EU, UNI-T, China) with an accuracy of ±0.01 kWh

3.4.2 Calculations

3.4.2.1. Salt Rejection

It is calculated from the following Equation (8) according to **Kucera, (2023):**

$$\text{Salt rejection } (\%) = \frac{\text{Feedwater conductivity} - \text{Permeate water conductivity}}{\text{Feedwater conductivity}} \quad (8)$$

3.4.2.2. Water recovery

It is calculated from the following Equation (9) according to **Kucera, (2023):**

$$\text{Water recovery}(\%) = \frac{\text{Permeate flow rate}}{\text{Feed flow rate}} \times 100 \quad (9)$$

3.5. Statistical Analyses

For statistical analyses, SPSS software (Version 20) was used. Paired t-tests were conducted to determine the significance of pressure values, electrical conductivity (EC) values, flow rate values, and sodium (Na) and chloride (Cl) concentrations between the first experiment (without EMF) and the second experiment (with EMF). Additionally, the standard deviation (SD) was calculated to assess the variability of the pressure measurements around their arithmetic mean.

RESULTS AND DISCUSSION

The effect of the electromagnetic field (EMF) on the performance of the reverse osmosis (RO) membrane was evaluated by measuring the salinity of the fresh water output, the salinity of the concentrated production, the pH values of fresh water and concentrated water, the pressure before the membrane, and the flow rate of freshwater, as well as calculating both the recovery rate and salt rejection.

The pH results in the first experiment for freshwater were 7.6, compared to the pH value of freshwater in the second experiment, which was 7.4. For concentrated water, the pH value in the first experiment was 8.7 and in the second experiment it was 8.5. A decrease in pH values was observed in the second experiment compared to the first experiment by 2.6% for freshwater and by 2.3% for concentrated water. This change is attributed to the effect of the electromagnetic field, which caused a higher concentration of hydrogen ions (H^+) in the material, making the freshwater and concentrated water more acidic in the second experiment.

Fig. (10) illustrates the pressure behavior before the membrane in both experiments. In the first experiment (without EMF), the pressure fluctuated between 420 and 460 kPa during most of the test period. However, during the final 18 hours, the pressure increased to 500 kPa, due to back pressure caused by partial clogging on the membrane surface.

In contrast, during the second experiment (with EMF), the pressure values remained within a narrower range, fluctuating between 440 and 480 kPa. The pressure measured after the RO membrane unit on the freshwater outlet line remained constant at 240 kPa in both experiments.

A strong, significant difference was observed in the pressure results between the first and second experiments. According to the standard deviation (SD) values shown on the pressure curves (Figure 10), the pressure readings in the second experiment were more stable than those

in the first. This stability is attributed to the effect of electromagnetic waves on the feed water prior to entering the membrane in the second experiment.

Fig. (11) shows that the average flow rate of freshwater in the first experiment was 0.1669 L/min over the 150-hour operating period, while in the second experiment it was 0.0988 L/min. The average flow rate in the second experiment was approximately 40.8% lower than that of the first experiment. This reduction in flow rate can be attributed to the blockage of pores within the flow channels of the reverse osmosis membrane elements. A statistically significant difference in flow rate was also observed between the two experiments, as illustrated in Fig. (11). Overall, the decline in flow rate in the second experiment supports the hypothesis of increased pore blockage within the membrane structure, due to the electromagnetic field treatment.

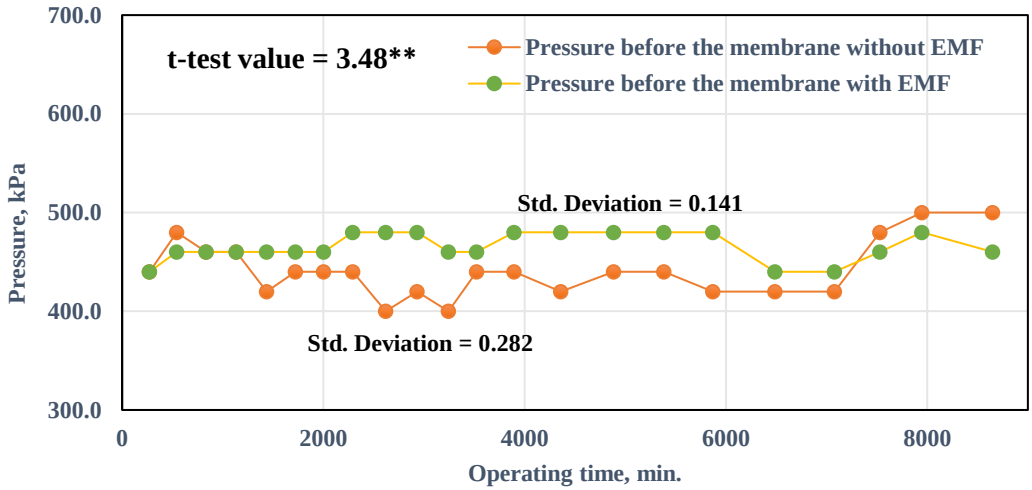

Fig. (10): Effect of operating time on the pressure before the membrane with and without EMF

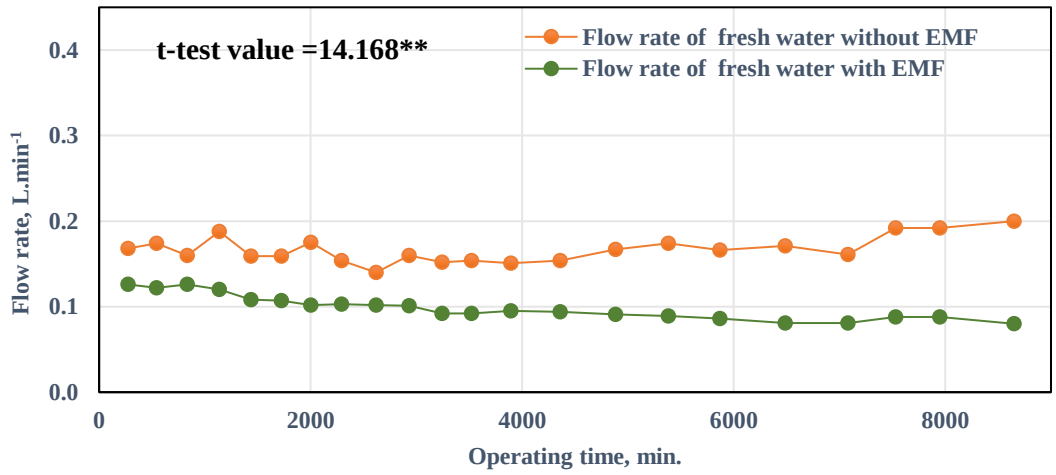

Fig. (11): Effect of operating time on flow rate for fresh water (with and without EMF)

Fig. (12) shows that the salinity of the freshwater output decreased over time in both experiments. In the first experiment (without EMF), salinity values declined from 0.30 $dS \cdot m^{-1}$ at the start to 0.24 $dS \cdot m^{-1}$ by the end of the 150-hour operating period. In the second experiment (with EMF), salinity values decreased more significantly, from 0.18 $dS \cdot m^{-1}$ to 0.08 $dS \cdot m^{-1}$ over

the same duration. The average salinity of freshwater in the second experiment was approximately 64% lower than in the first experiment. Regarding the concentrated water, the average salinity in the second experiment was approximately 15.6% lower than that of the first experiment. In the first experiment, the salinity of the concentrated water remained relatively constant throughout the test, averaging 5.8 $dS \cdot m^{-1}$. In contrast, the second experiment showed a gradual decrease in salinity, reaching 4.89 $dS \cdot m^{-1}$ by the end of the 150 hours, as illustrated in Fig. (13).

A strong, statistically significant difference was observed in electrical conductivity values of both freshwater and concentrated water between the two experiments, as shown in Fig. (12) and (13).

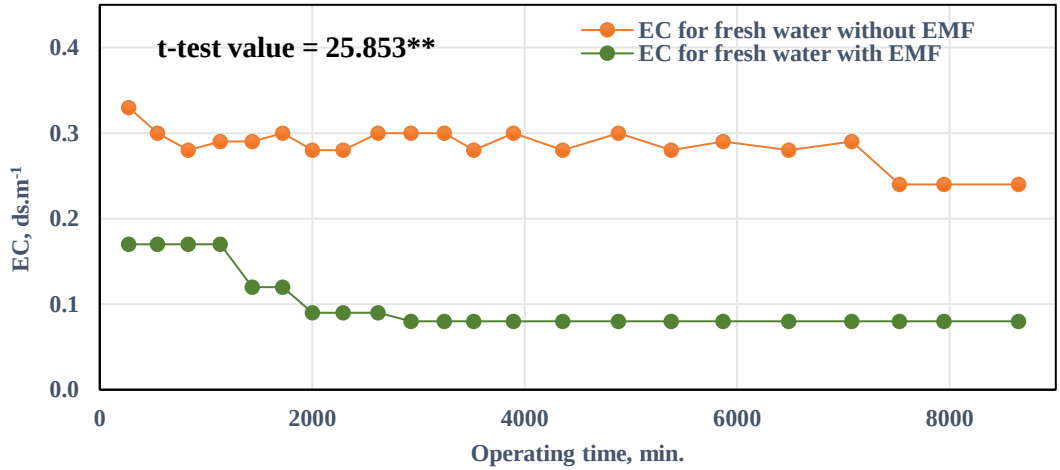

Fig. (12): Variation of Electrical Conductivity (EC) of Fresh Water with and Without EMF During the Operating Time of the Experiment

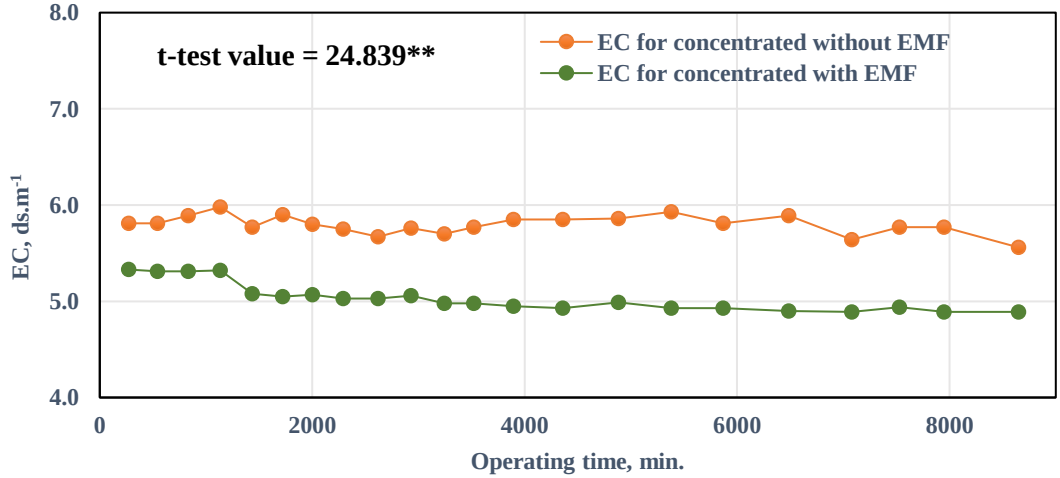

Fig. (13): Variation of Electrical Conductivity (EC) of Brine with and Without EMF During the Operating Time of the Experiment

Fig. (14) shows that the average dissolved sodium concentration in freshwater during the second experiment (with EMF) was approximately 19% lower than in the first experiment (without EMF).

Similarly, in the case of concentrated saline water, the average dissolved sodium in the second experiment was approximately 14% lower compared to the first experiment, as shown in Fig. (15).

Fig. (16) shows that the average concentration of dissolved chloride in freshwater during the second experiment (with EMF) was approximately 14% lower than in the first experiment (without EMF). Likewise, Fig. (17) shows that the average chloride concentration in concentrated saline water was approximately 46% lower in the second experiment compared to the first.

These results suggest that the electromagnetic field (EMF) may have enhanced the membrane's efficiency in separating and retaining ionic species. The EMF altered the behavior of dissolved ions, making them more susceptible to binding or interaction with the membrane material.

According to the paired t-test statistical analysis, the differences in sodium and chloride concentrations between the two experiments were found to be highly statistically significant:

- In freshwater, both sodium (Na^+) and chloride (Cl^-) concentrations showed very strong statistical significance, as shown in Fig. (14) and (16).
- In concentrated saline water, the differences in sodium and chloride concentrations were also highly significant, as shown in Fig. (15) and (17).

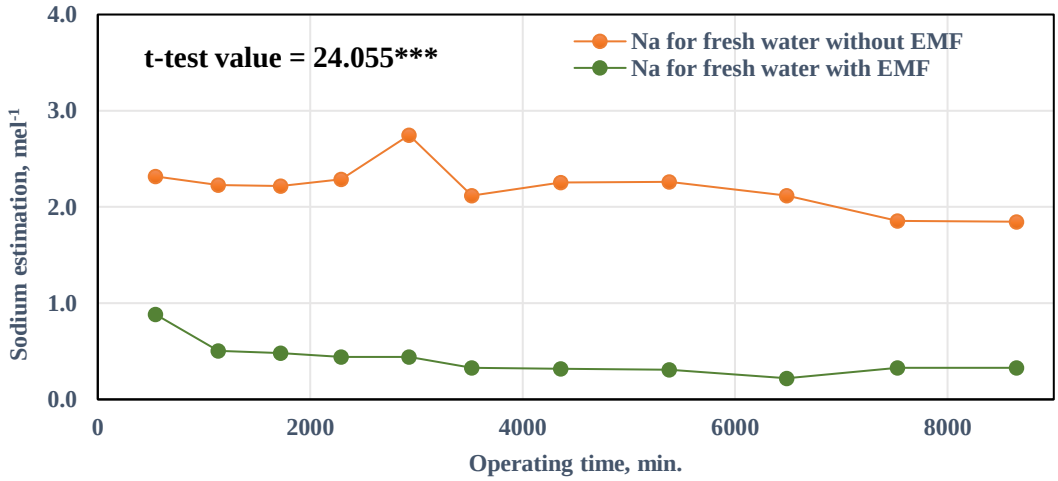

Fig. (14): Estimation of Sodium Concentration in Freshwater with and Without Electromagnetic Field (EMF)

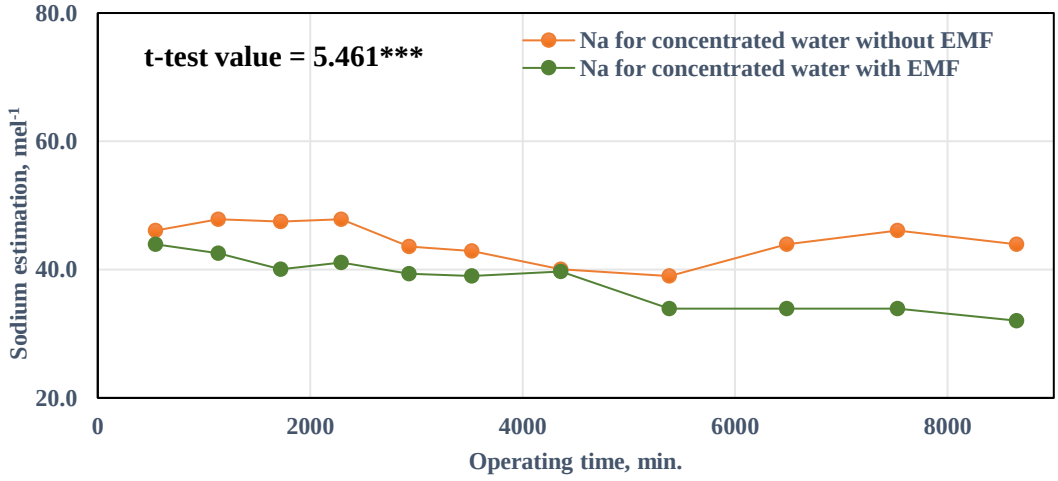

Fig. (15): Estimation of Sodium Concentration in Brine with and Without Electromagnetic Field (EMF)

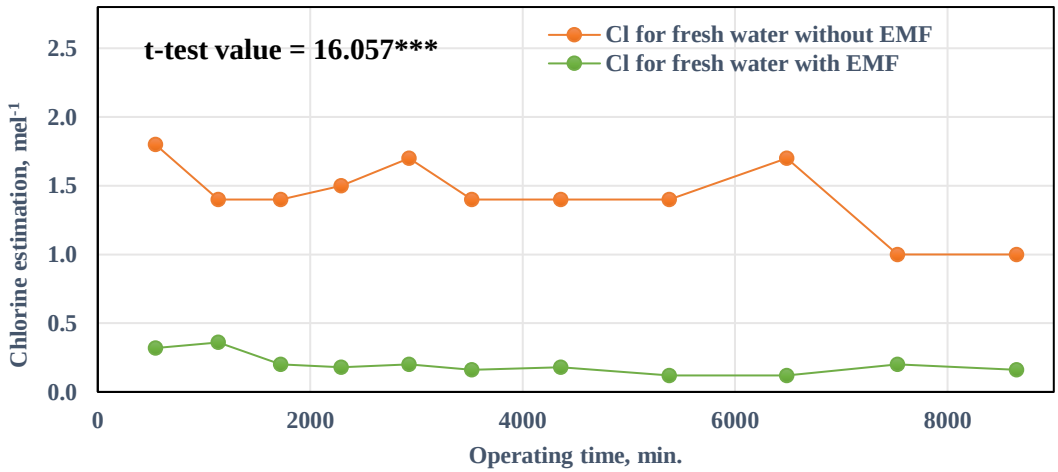

Fig. (16): Estimation of Chloride Concentration in Freshwater with and Without Electromagnetic Field (EMF)

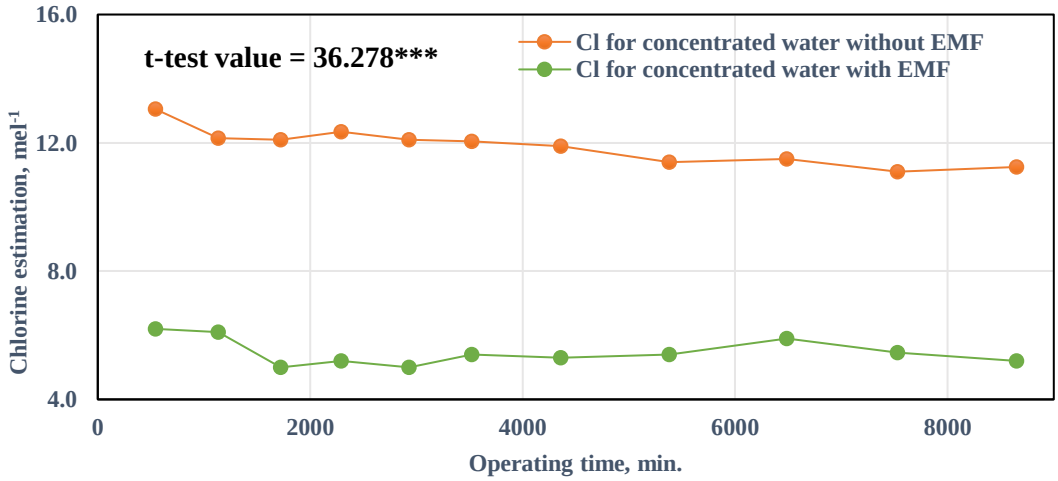

Fig. (17): Estimation of Chloride Concentration in Brine with and Without Electromagnetic

According to the previous results, the observed decrease in salinity, as well as the reduction in dissolved sodium and chloride concentrations in the second experiment (with EMF) compared to the first (without EMF), can be attributed to the effect of electromagnetic field (EMF) treatment.

The EMF appears to have enhanced the deposition of scale on the membrane surface, resulting in partial blockage of the membrane pores. This, in turn, resulted in a decrease in flow rate and electrical conductivity in the second experiment compared to the first..

Table 2: Values of Recovery Rate, Salt Rejection Rate, and Energy Consumption for Both Experiments

Treatment	Recovery rate (%)	Salt rejection rate (%)	Energy consumption (kWh)
Without (EMF)	16.7	92.8	0.031
With (EMF)	9.9	97.5	0.034

The increase in salt rejection values of the membrane in the second experiment, as shown in Table (2), indicates that the system was more effective in blocking dissolved impurities when EMF treatment was applied. A decrease in salt rejection rate may indicate an increase in membrane fouling, which can affect salt removal. This enhancement also explains the observed reduction in the salinity of the freshwater output compared to the first experiment (without EMF).

On the other hand, the recovery rate values presented in Table (2) show that the membrane in the first experiment converted a larger percentage of the feed water into freshwater than in the second experiment. This suggests that the application of EMF led to a reduction in freshwater yield and a corresponding increase in the volume of concentrated brine, due to the reduced flow rate observed in the second experiment.

These findings suggest that the **electromagnetic field (EMF)** enhanced the membrane's efficiency in **separating and retaining dissolved elements**. The EMF may have altered the physical or chemical properties of the ions, making them **more likely to bind** with the membrane surface.

As shown in **Table (2**), the **energy consumption** in the **second experiment (with EMF)** was approximately **8% higher** than in the **first experiment (without EMF)**.

Based on the **electricity rate in Egypt (2 E.P./kWh)** (**MOERE., 2025**), the **estimated energy cost** for operating the system was over 150 hours, **9.38 E.P.** for the first experiment and **10.14 E.P.** for the second experiment.

CONCLUSSION

This research aimed to investigate the effect of an electromagnetic field on the performance of reverse osmosis membranes. Two experiments were conducted, each lasting 150 hours. The first experiment evaluated the membrane's performance without any exposure to the electromagnetic field. In contrast, the second assessed its performance under the influence of an electromagnetic field applied before the membrane at a frequency of 150 kHz. A helical coil was wound and connected to a circuit designed to generate this frequency. The circuit included an operational amplifier (Op-Amp), a network of passive components (Wien Bridge Oscillator), a comparator, and a power amplifier. This setup was used to generate the electromagnetic field and apply it prior to the reverse osmosis unit.

The findings of this research can be summarized as follows:

1. A significant difference was observed in pressure measurements before the reverse osmosis unit over 150 hours. The pressure in the second experiment was more stable compared to the first, as indicated by lower standard deviation values.
2. A noticeable decrease in the discharge of fresh effluent water was recorded in the second experiment compared to the first. Consequently, the recovery rate in the second experiment was lower than that in the first.
3. The salinity of the freshwater output, along with the concentrations of dissolved sodium and chloride, decreased in the second experiment compared to the first. As a result, the salt rejection rate of the membrane in the second experiment was higher than in the first.

These findings indicate that the application of an electromagnetic field improved the membrane's performance in salt separation.

REFERANCES

Alwan, A. A., Ahmed, S., Nwokoye, A., Alhendi, A. A., Ibrahim, O., and Alhseinat, E. (2024). Recent advances in the application of magnetic/electromagnetic field for water desalination. *Current Trends and Future Developments on (Bio-) Membranes*, 427-459. https://doi.org/10.1016/B978-0-323-99311-1.00010-6

Antony, A., Low, J. H., Gray, S., Childress, A. E., Le-Clech, P., and Leslie, G. (2011). Scale formation and control in high-pressure membrane water treatment systems: A review. Journal of membrane science, 383(1-2), 1-16. https://doi.org/10.1016/j.memsci.2011.08.054

Bisbee, D. (2003). Pulse-Power Water Treatment Systems for Cooling Towers. *Energy Efficiency & Customer Research & Development Sacramento Municipal Utility District*.

Beaty, H. W. (2001). Chapter One, Basic Network Analysis, HANDBOOK OF ELECTRIC POWER CALCULATIONS. McGraw-Hill Professional, New York, pp. 14-16, 19 and 23-27

Chase, D. V. (2022). Chapter Four, Volumetric Flowrate, Velocity and the Continuity Equation, Open Educational Resource: Civil Engineering Course Notes. Pp. 182.

Chen, L., Xu, P., and Wang, H. (2020). Interplay of the factors affecting water flux and salt rejection in membrane distillation: A state-of-the-art critical review. *Water*, *12*(10), 2841. https://doi.org/10.3390/w12102841

Conway, J.M. (2002). Electronic Scale Treatment, a Commercial and Industrial Article, Clear Water Enviro Technologies, Available from: http://www.wqpmag.com/sites/default/files/_P.14-16%20Scale%204_02.pdf

Du, X., Perera, H., Ahasan, T., Wang, Y., Shu, F., Wang, H., ... and Xu, P. (2025). Mechanisms of electromagnetic field control on mineral scaling in brackish water reverse osmosis: Combined homogenous and heterogeneous nucleation. *Separation and Purification Technology*, *355*, 129630. DOI: 10.1021/acs.est.4c14658

Du, X., Jiang, W., Wang, Y., Shu, F., Wang, H., Vazquez, D., ... and Xu, P. (2024). Numerical modeling of electromagnetic field spatiotemporal evolution to evaluate the effects on calcium carbonate crystallization. *Desalination*, *592*, 118128. https://doi.org/10.1016/j.desal.2024.118128

Geise, G. M., Lee, H. S., Miller, D. J., Freeman, B. D., McGrath, J. E., and Paul, D. R. (2010). Water purification by membranes: the role of polymer science. *Journal of Polymer Science Part B: Polymer Physics*, *48*(15), 1685-1718. https://doi.org/10.1002/polb.22037

Greenlee, L. F., Lawler, D. F., Freeman, B. D., Marrot, B., and Moulin, P. (2009). Reverse osmosis desalination: water sources, technology, and today's challenges. Water research, 43(9), 2317-2348. https://doi.org/10.1016/j.watres.2009.03.010

Huchler, L. A., Mar, P. E., and Lawrenceville, N. J. (2002, October). Non-chemical water treatment systems: histories, principles and literature review. In International Water Conference (pp. 02-45). Available from: https://www.thomasnet.com/pdf.php?prid=100429

Kucera, J. (2023). Chapter two, Principles and Terminology, *Reverse osmosis*. John Wiley & Sons. Pp. 35 and 38.

Lee, H. J., Halali, M. A., Baker, T., Sarathy, S., and de Lannoy, C. F. (2020). A comparative study of RO membrane scale inhibitors in wastewater reclamation: Antiscalants versus pH adjustment. *Separation and Purification Technology*, *240*, 116549. https://doi.org/10.1016/j.seppur.2020.116549

Lee, J., Ren, X., Yu, H. W., Kim, S. J., and Kim, I. S. (2010). Membrane biofouling of seawater reverse osmosis initiated by sporogenic Bacillus strain. Environmental Engineering Research, 15(3), 141-147. https://doi.org/10.4491/eer.2010.15.3.141

Lin, L., Jiang, W., Xu, X., and Xu, P. (2020). A critical review of the application of electromagnetic fields for scaling control in water systems: mechanisms, characterization, and operation. *NPJ Clean Water*, *3*(1), 25. https://doi.org/10.1038/s41545-020-0071-9

MOERE, (2025). Ministry of Electricity and Renewable Energy.

Matin, A., Laoui, T., Falath, W., and Farooque, M. (2021). Fouling control in reverse osmosis for water desalination & reuse: Current practices & emerging environment-friendly technologies. *Science of the Total Environment*, *765*, 142721. https://doi.org/10.1016/j.scitotenv.2020.142721

Nair, M., and Kumar, D. (2013). Water desalination and challenges: The Middle East perspective: a review. *Desalination and Water Treatment*, *51*(10-12), 2030-2040. https://doi.org/10.1080/19443994.2013.734483

Pearson, J. L., Michael, P. R., Ghaffour, N., and Missimer, T. M. (2021). Economics and Energy Consumption of Brackish Water Reverse Osmosis Desalination: Innovations and Impacts of Feedwater Quality. *Membranes*, *11*(8), 616. https://doi.org/10.3390/membranes11080616

Penteado de Almeida, J., Stoll, Z., and Xu, P. (2023). An Alternating, Current-Induced Electromagnetic Field for Membrane Fouling and Scaling Control during Desalination of Secondary Effluent from Municipal Wastewater. *Water*, *15*(12), 2234. https://doi.org/10.3390/w15122234

Razavi, B. (2021). Fundamentals of Microelectronics. John Wiley & Sons, pp. 381-384 and 660-661

Saksono, N., Bismo, S., Widaningroem, R., and Manaf, A. (2011). Formation of CaCO3 particle and conductivity of Na2CO3 and CaCl2 solution under magnetic field on dynamic fluid system. *Makara Journal of Technology*, *15*(1), 14. https://doi.org/10.7454/mst. v15i1.862.

Sheikholeslami, R. (2004). Assessment of the scaling potential for sparingly soluble salts in RO and NF units. Desalination, 167, 247-256. https://doi.org/10.1016/j.desal.2004.06.134

Schoenbach, K. H., Alden, R. W., and Fox, T. J. (1996, June). Biofouling prevention with pulsed electric fields. In Proceedings of 1996 International Power Modulator Symposium (pp. 75-78). IEEE. 10.1109/MODSYM.1996.564454

Skoog D. A.; West D. M., and Holler F. J. (1996). Fundamentals of Analytical Chemistry, 7th Edition, Thomson Learning, Inc, USA.

Taherinejad, M., Derakhshan, S., and Yavarinasab, A. (2017). Hydrodynamic analysis of spiral wound reverse osmosis membrane recovery fraction and permeate water flow rate. *Desalination, 411*, 59-68. https://doi.org/10.1016/j.desal.2017.02.009

Thompson, J., Lin, N., Lyster, E., Arbel, R., Knoell, T., Gilron, J., and Cohen, Y. (2012). RO membrane mineral scaling in the presence of a biofilm. Journal of Membrane Science, 415, 181-191. https://doi.org/10.1016/j.memsci.2012.04.051

Rouina, M., Kariminia, H. R., Mousavi, S. A., and Shahryari, E. (2016). Effect of electromagnetic field on membrane fouling in reverse osmosis process. *Desalination, 395,* 41-45. https://doi.org/10.1016/j.desal.2016.05.009

تأثير استخدام مجال كهرومغناطيسي على أداء أغشية التناضح العكسي في المياه متوسطة الملوحة

سلوى طارق عبد العزيز[١]، أسامة محمد احمد بدير[٢]، عمرو مسعد[٢]، حمدي السيسي احمد[٣]، كريم مصطفى السواح[٤]، أنس محمد محمود سلامه[٥]

[١] طالبة ماجستير بقسم الهندسة الزراعية - كلية الزراعة - جامعة عين شمس – القليوبية – مصر.
[٢] استاذ بقسم الهندسة الزراعية - كلية الزراعة - جامعة عين شمس – القليوبية – مصر.
[٣] مستشار رئيس مجلس ادارة مصنع المحركات الهيئة العربية للتصنيع - القاهرة – مصر.
[٤] مهندس إلكترونيات حر– القاهرة – مصر.
[٥] مدرس بقسم علوم الاراضى - كلية الزراعة - جامعة عين شمس – القليوبية – مصر.

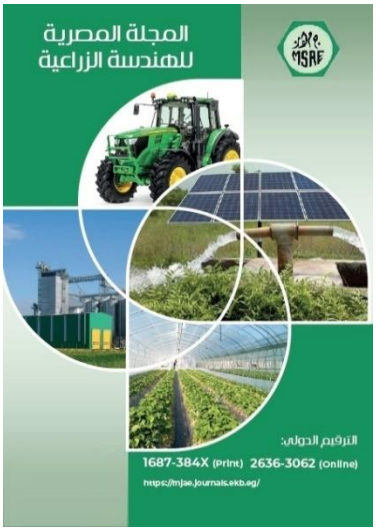

© **المجلة المصرية للهندسة الزراعية**

الكلمات المفتاحية:
التحلية؛ مياه متوسطة الملوحة؛ التناضح العكسي؛ التكلس؛ المجال الكهرومغناطيسي؛ مولد التردد؛ معدل استرداد المياه؛ معدل رفض الملح؛ تقدير العناصر

الملخص العربى

لطالما اعتُبرت أغشية التناضح العكسي من أكثر الوسائل شيوعًا وفعالية في تحلية المياه، نظرًا لسهولة تشغيلها وكفاءتها العالية في فصل الأملاح. ومع ذلك، يُعد التكلّس أحد أبرز التحديات التي تواجه هذه الأغشية، إذ يمكن أن يؤدي إلى انخفاض معدل التدفق وتلف الغشاء. ومن هذا المنطلق، أصبح استخدام المجال الكهرومغناطيسي خلال العقود الأخيرة من الطرق الشائعة في معالجة المياه.

اعتمدت هذه الدراسة على تجربتين: الأولى بدون تطبيق مجال كهرومغناطيسي قبل الغشاء، والثانية مع تطبيق المجال الكهرومغناطيسي قبله. وقد أُجريت التجارب في مختبر الأبحاث التابع لقسم علوم التربة والمياه، بكلية الزراعة – جامعة عين شمس. وهدفت الدراسة إلى تقييم تأثير المجال الكهرومغناطيسي الذي تم توليده باستخدام ملف حلزوني من الأسلاك الموصولة بدائرة إلكترونية لتوليد تردد قدره ١٥٠ كيلوهرتز.

وقد أظهرت نتائج التجربة تحسّنًا في أداء الغشاء، تمثل في زيادة معدل رفض الأملاح في المياه المنتجة، وانخفاض تركيز أيونات الصوديوم والكلوريد في المياه العذبة والمياه المركزة، كما أظهرت النتائج انخفاضًا في معدل استرداد المياه العذبة.